Clinical Radiology 74 (2019) 407.e11–407.e17

Contents lists available at ScienceDirect

Clinical Radiology

journal homepage: www.clinicalradiologyonline.net

Assessment of liver cirrhosis for patients with Child's A classification before hepatectomy using dynamic contrast-enhanced MRI

Y.-S. Liao [a,b,c], L.-W. Lee [b,d], P.-H. Yang [c], L.-M. Kuo [e], L.-Y. Kuan [d], W.-Y.I. Tseng [f], D.W. Hwang [c,g,h,*]

[a] Department of Diagnostic Radiology, Chang Gung Memorial Hospital, Yunlin, Taiwan
[b] Department of Nursing, Chang Gung University of Science and Technology, Chiayi, Taiwan
[c] Department of Chemistry and Biochemistry, National Chung Cheng University, Chiayi, Taiwan
[d] Department of Diagnostic Radiology, Chang Gung Memorial Hospital, Chiayi, Taiwan
[e] Department of General Surgery, Chang Gung Memorial Hospital, Chiayi, Taiwan
[f] Institute of Medical Device and Imaging, National Taiwan University College of Medicine, Taipei, Taiwan
[g] Center for NanoBiodetection, National Chung Cheng University, Chiayi, Taiwan
[h] Institute of Biomedical Sciences, Academia Sinica, Taipei, Taiwan

ARTICLE INFORMATION

Article history:
Received 13 August 2018
Accepted 23 January 2019

AIM: To determine the feasibility of semi-quantitative haemodynamic parameters derived from dynamic contrast-enhanced (DCE) magnetic resonance imaging (MRI) to assess liver fibrosis.

MATERIALS AND METHODS: Seventy-five patients with Child's A classification (males/females=24/51; average age, 58 years; range, 30–80 years) received DCE-MRI 3 days prior to hepatectomy. Semi-quantitative haemodynamic parameters, including the wash-in slope, wash-out slope, and time-to-peak, were calculated from DCE-MRI data. Liver fibrosis of the resected non-tumour liver was graded pathologically from F0 (no fibrosis) to F6 (cirrhosis) in the regions corresponding to those assessed by DCE-MRI.

RESULTS: The wash-out slope showed higher interobserver and intra-observer reliabilities than the wash-in slope and time-to-peak. There was a significant positive correlation between the wash-out slope and pathological grade of fibrosis (Spearman's correlation coefficient: r=0.5331, p<0.0001). The area under the receiver operating characteristic curve was 0.8066 when using the wash-out slope to differentiate cirrhosis (grade F6) from non-cirrhosis (grades F0–5). Using the cut-off point that maximised specificity, the sensitivity was 62.07%, specificity was 91.30%, positive predictive value was 81.81%, negative predictive value was 79.25%, and accuracy was 80%.

CONCLUSIONS: The wash-out slope derived from DCE-MRI might be potentially useful in assessing liver cirrhosis in patients with Child's A classification before hepatectomy.

* Guarantor and correspondent: D. W. Hwang, Institute of Biomedical Sciences, Academia Sinica, No 128, Sec. 2, Academia Rd, Nangang, Taipei 11529, Taiwan. Tel.: +886 2 27899027; fax: +886 2 27887641.
E-mail address: dwhwang@ibms.sinica.edu.tw (D.W. Hwang).

https://doi.org/10.1016/j.crad.2019.01.017
0009-9260/

Introduction

Liver fibrosis is a common process in chronic liver disease, which leads to compromised liver function. Following liver injury, the recruitment of immune cells is followed by the activation of hepatic stellate cells. Hepatic stellate cells produce excessive extracellular matrix proteins, and generate temporary scars to protect the liver from further injury. The excessive protein matrix in the space of Disse blocks endothelial fenestration, a process called sinusoidal capillarisation, leading to hypoperfusion of the hepatocytes.[1] In addition, activated hepatic stellate cells secrete cytokines and growth factors to promote nodular regeneration surrounding the fibrotic scars, resulting in distortion of the hepatic microstructure, and increased resistance to portal blood flow.[2,3]

Hepatic failure is a major cause of morbidity and mortality after liver resection. Assessment of liver function before surgery is critical in cirrhotic patients who require extended hepatectomy, and those who are potential living donors. Currently, common indicators of surgical risk for hepatectomy include the Child–Pugh score, indocyanine green retention test, aspartate aminotransferase to platelet ratio index, and computed tomography (CT) volumetry.[4,5] Although laboratory-based tests can assess overall liver function, they are limited in predicting liver reserve after surgery. CT volumetry can only assess the volume, and not the function of the remaining liver, and cannot provide information about the severity of liver fibrosis. Quantitative imaging of liver fibrosis is desirable to accurately assess the extent of liver fibrosis after liver resection.

There are several methods for assessing liver fibrosis, including liver biopsy, serum markers, and non-invasive imaging. Liver biopsy analysis is considered the reference standard for staging hepatic fibrosis; however, it is limited by small specimen size, sampling variability, and invasiveness.[6] These limitations make liver biopsy a less than ideal reference standard.[7] Conventional liver functional tests and serum makers reflect the general status of the hepatobiliary system, rather than the degree of liver fibrosis, and therefore, may not be suitable for staging liver fibrosis. Magnetic resonance imaging (MRI) is a non-invasive imaging tool that is free of ionising radiation. A MRI technique that can assess the extent of liver fibrosis in the residual liver prior to hepatectomy would be of value.

Dynamic contrast-enhanced (DCE) magnetic resonance imaging (MRI) has been validated for the assessment of angiogenesis and tissue perfusion.[8–10] As liver fibrosis is characterised by increased intrahepatic vascular resistance and decreased exchange between the sinusoids and hepatocytes,[11] it may be assessed by DCE-MRI; however, the analysis of DCE-MRI for liver fibrosis usually invokes complex mathematical modelling and lengthy data processing, thereby its clinical use is uncommon. Moreover, the unique dual blood supplies of the liver and the presence of intrahepatic vascular shunts further complicate the analysis.[12–14] Therefore, the aim of the present study was to investigate the feasibility of using a semi-quantitative index derived from DCE-MRI to assess the degree of liver fibrosis for patients with Child's A classification before hepatectomy.

Materials and methods

Patients

The study was approved by the Local Institutional Review Board of Chang Gung Memorial Hospital (CGMH101-4766A3). All patients provided written informed consent before entering the study. From July 2013 to February 2015, all patients with Child's A classification who were scheduled to receive hepatectomy at Chang Gung Memorial Hospital were invited to participate in the study. Exclusion criteria included age <20 years, impaired renal function (defined as an estimated glomerular filtration rate [eGFR] <30 ml/min/1.73 m^2), and standard MRI contraindications, including patients who had implants incompatible with MRI, pregnancy, claustrophobia, and jewellery piercings.

Ninety-four patients were recruited, and all of them were Child's A classification. Three refused surgery, and were thus excluded. Four were excluded because of liver disease that might confound the analysis: two had severe liver steatosis, one had a giant hepatic haemangioma, and one had severe hepatitis. One who did not have enough non-tumour liver tissue for pathological grading of liver fibrosis was also excluded. Seven patients were also excluded owing to enhancement failure such as: prolonged time-to-peak (n=3) with very short wash-out curve and absence of wash-out (n=4) mimicking "dripping" enhancement. Four patients were excluded due to atypical MRI signal enhancement (n=4). Consequently, 24 females (average age, 53 years; age range, 41–79 years) and 51 males (average age, 60 years; range, 30–80 years) were included in the analysis.

MRI protocol

All MRI studies were acquired within 3 days prior to hepatectomy. DCE-MRI studies were performed on a 3 T MRI system (Verio, Siemens, Erlangen, Germany) with a six-channel phased-array body coil. A three-dimensional (3D)-volumetric interpolated breath-hold examination (VIBE) sequence was used with the imaging parameters as follows: 4.76 ms repetition time, 1.32 ms echo time, 32.5×40 cm field of view, 208×256 matrix, 4.25 mm section thickness, 15° flip angle, 12 sections in coronal view, 1.56×1.56×4.25 mm^3 image resolution, and 2.525 second temporal resolution.

Based on DCE-MRI guidelines, the dynamic imaging protocol entailed 120 consecutive acquisitions over a period of 303 seconds (Fig 1).[15] At the 10^{th} acquisition, gadolinium diethylenetriamine-pentaacid (Gd-DTPA, Magnevist, Bayer Schering Pharma AG, Berlin, Germany) at a dosage of 0.2 mmol/kg of body weight was administered intravenously at a rate of 3 ml/s through an MRI-compatible power injector (Optistar Elite Injector, Covidien, Cincinnati, OH, USA), followed by a 20 ml saline flush at the same rate. Patients were coached to perform shallow breathing throughout the entire examination.

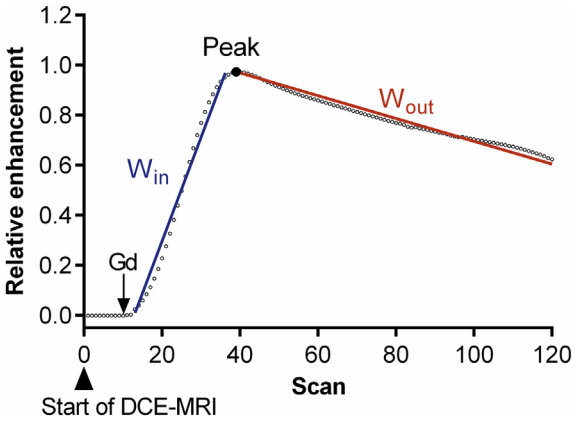

Figure 1 The time curve of dynamic contrast enhancement acquired by DCE-MRI. Gd-DTPA (0.2 mmol/kg body weight) was given intravenously at the 10th scan. Scanning continued until a total of 120 consecutive acquisitions were completed. Time-to-peak, the wash-in slope (W_{in}), and the wash-out (W_{ou}) slope were defined on the normalised dynamic contrast enhancement curve.

Region of interest selection

Prior to the study, two radiologists with >10 years of experience in liver imaging were trained on the criteria of selecting the region of interest (ROI) on DCE-MRI in a trial of 10 subjects. The ROI was selected to fit the region from which a non-tumour liver sample was taken during surgery for liver fibrosis staging. Regions showing visible bile ducts and blood vessels, and regions close to diaphragm, were avoided. The radiologists selected the ROIs independently, and were blinded to the clinical information and pathological stage of liver fibrosis. Prior to ROI selection, the image stabilisation program[16] was used to minimise motion artefact. A single ROI was drawn for each patient, and was copied and pasted on the same section location for all time points using Image J software (Image J 1.3.1, NIH, Maryland, USA). The selected ROI was 119±45mm^2 in size. Two radiologists measured all the DCE-MRI scans separately to examine interobserver reliability. Rater 1 repeated all the ROI selections 3 months later to evaluate intra-rater reliability.

Image analysis

For each dataset, the baseline signal intensity (SI_0) was defined as the mean signal intensity of the first 10 scans of the time–intensity curve. Relative contrast enhancement at each time point ($SI_{relative}$) was calculated as:

$$SI_{relative}=(SI_t - SI_0)/SI_0 \times 100\%,$$

where SI_t was the signal intensity at frame t after the start of DCE-MRI.

To reduce the noise, the data points of the time–intensity curve were smoothed by a weighted 10 points using the fast Fourier transform algorithm (OriginPro 8.1 SR1, OriginLab, Northampton, MA, USA), and was normalised by scaling the signal intensity between 0 and 1. As shown in Fig 1, the time–intensity curve showed a rapid increase in signal intensity soon after administration of the contrast medium bolus, reaching the peak, and then a slow decline. The peak signal intensity was defined as the maximum value of the normalised time–intensity curve. The wash-in and wash-out slopes of the time–intensity curve were determined using a linear regression model (line of best fit). The following parameters were calculated[1]: time-to-peak, the time interval from the onset of enhancement to peak signal intensity[2]; the wash-out slope, the slope between the peak signal intensity and the cut-off times of 180, 210, 240, 270, and 300 seconds from the start of dynamic scanning[3]; the wash-in slope, the slope between the onset of enhancement and the peak signal intensity.[17]

Histopathological examination

Non-tumour liver specimens were formalin-fixed, paraffin-embedded, and stained with haematoxylin and eosin. Each sample was evaluated histologically according to Ishak staging.[18] Ishak staging has seven scores from F0 to F6, which indicate different degrees of liver fibrosis; F0: no fibrosis, F1: fibrous expansion of some portal areas, F2: fibrous expansion of most portal areas, F3: fibrous expansion of most portal areas with occasional portal to portal bridging, F4: fibrous expansion of portal areas with marked bridging, F5: marked bridging with occasional nodules, and F6: probable or definite cirrhosis.

Statistical analysis

Differences among groups were tested using one-way ANOVA with Bonferroni correction for multiple comparisons. A probability (p) value of <0.05 was considered statistically significant. The interobserver reliability and intra-observer reliability were evaluated in terms of intra-class correlation coefficient (ICC).[19] Spearman's correlation coefficient was used to evaluate the correlations between the wash-out slope and Ishak stage. The area under the receiver operating characteristic (AUC) curve was used to quantify the overall ability of the DCE-MRI parameters to discriminate cirrhosis (F6) and non-cirrhosis (F0–F5), and curves were calculated using PRISM6 software (GraphPad Software, San Diego, CA, USA).

RESULTS

A total of 75 patients were included in the final analysis, and were divided into three subgroups according to the Ishak staging (20). There were 20 patients with mild liver fibrosis (stage F0–3), 26 patients with moderate fibrosis (F4–5), and 29 patients with cirrhosis (F6). The demographic data of these 75 patients are shown in Table 1. The proportion of patients with hepatitis B and/or hepatitis C increased as the degree of liver fibrosis increased (mild fibrosis: 9/20; moderate fibrosis: 23/26; cirrhosis: 27/29). The signal intensity (mean with standard deviation) profiles of non-tumour liver parenchyma following contrast medium injection of the three subgroups are shown in Fig 2. Although the wash-out slopes of mild and moderate liver

Table 1
Patient characteristics.

Ishak stage	No. of patients	Age (years)	M/F	Hepatitis virus infection			
				B	C	B and C	None
F0–3	20	63.75±9.87	12/8	5	2	2	11
F4–5	26	58.58±11.14	22/4	13	7	3	3
F6	29	61.52±10.33	17/12	13	11	3	2

Data are presented as mean ± standard deviation or number.

Table 2
Intra-observer and interobserver reliabilities of DCE-MRI parameters as indicated by intra-class correlation coefficients.

	Time-to-peak	Wash-in slope	Wash-out slope at different cut-off times				
			300 s	270 s	240 s	210 s	180s
Intra-observer	0.58	0.50	0.76	0.85	0.86	0.89	0.92
interobserver	0.52	0.53	0.73	0.72	0.73	0.80	0.80

fibrosis were indistinguishable, that of liver cirrhosis was obviously slow.

The intra-observer and interobserver reliabilities of time-to-peak, wash-in slope, and wash-out slope with the cut-off times of 180, 210, 240, 270, and 300 seconds are summarised in Table 2. Among all parameters, the wash-out slope at the 180-second cut-off showed the highest intra-observer reliability (ICC=0.92) and interobserver reliability (ICC=0.80).

The area under the receiver operating characteristic curve analysis of the wash-out slopes at different cut-off times of 180, 210, 240, 270, and 300 seconds for differentiating cirrhosis (F6) from non-cirrhosis (F0–F5) is shown in Table 3. Among all cut-off times, the wash-out slope at the 180-second cut-off time showed the largest AUC (0.8066). A high correlation was observed between the wash-out slopes at the 180-second cut-off and Ishak fibrosis stage (Fig 3). The Spearman's correlation was significant (r=0.5331, p<0.0001).

Fig 4 shows the ROC analyses of the wash-out slope at the 180-second cut-off in differentiating cirrhosis (F6) from non-cirrhosis (F0–F5). The AUC was 0.8066. Using the cut-off point that maximised specificity (wash-out slope=−0.002437 1/second), the sensitivity was 62.07%, specificity was 91.3%, positive predictive value (PPV) was 81.81%, negative predictive value (NPV) was 79.25%, and accuracy was 80% for differentiating cirrhosis from non-cirrhosis.

Fig 5 is the mean, standard deviation, maximum, and minimum plots of 180-second washout slopes at different fibrosis stages. There are significant difference of washout slopes between F0–3 and F6 (p<0.0001), and also F4–5 and F6 (p<0.001).

Discussion

To the authors' knowledge, this is the first MRI study to assess liver fibrosis in patients with Child's A classification prior to hepatectomy. In this study, a metric was determined to assess the severity of liver fibrosis based on semi-quantitative parameters derived from DCE-MRI. Among all parameters, the wash-out slope at the 180-second cut-off showed the highest intra-observer and interobserver reliabilities. When compared with the pathological grade of liver fibrosis, the magnitude of the wash-out slope decreased with increasing severity of liver fibrosis, and it had the largest AUC in distinguishing liver cirrhosis from non-cirrhosis. The overall accuracy was 80%, with a specificity of 91.3% and PPV of 81.81%. Owing to its ease of use and acceptable diagnostic accuracy, the wash-out slope might be a feasible metric for assessing the severity of liver fibrosis.

The high specificity (91.3%) and high PPV (81.81%) of the proposed wash-out slope have important clinical implications. When surgeons perform hepatectomy, they are most concerned about liver function reserve after hepatic resection. The high PPV means that when non-tumour liver tissue is diagnosed to be cirrhotic, the chance of it actually being cirrhotic is >81%. The high specificity means that in

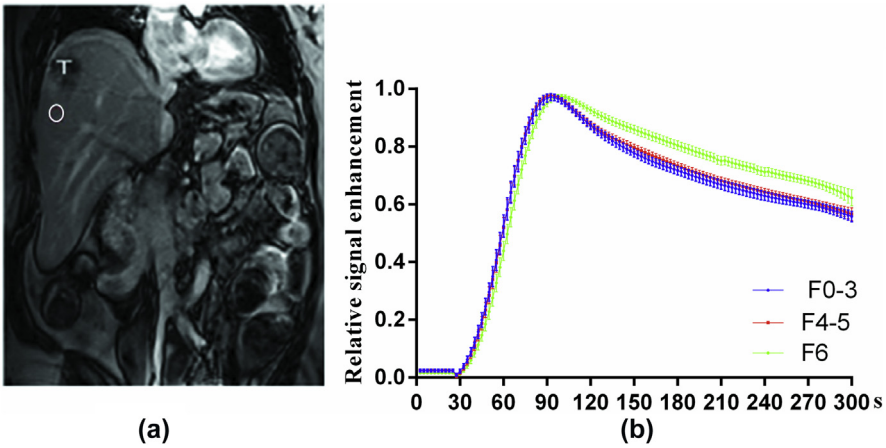

Figure 2 (a) A patient with a hepatic tumour (T) in right upper liver. A circle was drawn as the region of interest in a non-tumour region. (b) Time–signal curves of non-tumour liver parenchyma following contrast medium injection in patients with mild liver fibrosis (F0–3), moderate fibrosis (F4–5), and cirrhosis (F6). The error bars are ±1 standard deviations.

Table 3
Area under the receiver operating characteristic curve in distinguishing liver cirrhosis (Ishak stage F6) from non-cirrhosis (Ishak stage F0–F5) using the wash-out slopes at different cut-off times.

Cut-off time	300 s	270 s	240 s	210 s	180 s
AUC	0.7466	0.7732	0.7736	0.7916	0.8066
p value	0.0003	<0.0001	<0.0001	<0.0001	<0.0001

AUC, area under the receiver operating characteristic curve.

patients without cirrhosis, the chance of being falsely diagnosed to be cirrhotic is <9%. This diagnostic performance indicates that the wash-out slope has high accuracy in diagnosing liver cirrhosis. When hepatectomy is performed on patients with cirrhosis, there is a greater risk of hepatic failure after surgery, especially when the resected volume is large. On the other hand, a low sensitivity would have a high false-negative rate; therefore, the wash-out slope at the cut-off point with high specificity is not suitable for screening.

In the present study, liver fibrosis was staged using the Ishak scale, which uses descriptive categories instead of quantitative scales.[18] Some studies have demonstrated a positive correlation between measured collagen proportionate areas and Ishak fibrosis scores.[20,21] Those studies showed that liver collagen amount increased exponentially, not linearly, with increasing Ishak scores. Compared with these results, the present study showed that there was a marked increase of the wash-out slope in the cirrhosis group (F6), and little difference between mild (F0–3) and moderate (F4–5) fibrosis (Figs 3 and 5). Similarly, Fig 2 shows flattening of the signal decline in the wash-out phase in the cirrhosis group, whereas the signal decline become relatively steeper in the mild and moderate fibrosis groups. This suggests that the wash-out slope of DCE-MRI might be an effective marker of liver cirrhosis.

Unlike perfusion MRI studies of the brain, there is no generally accepted model for analysing hepatic DCE-MRI data sets because of the dual blood supplies in the liver. The Marterne model is the most popular DCE-MRI model for the liver, which extracts perfusion fractions from the hepatic arteries and portal veins within the liver[22]; however, it cannot model the change in permeability between

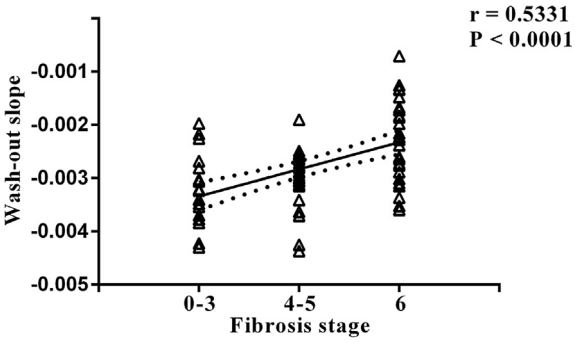

Figure 3 Correlation between the wash-out slope and liver fibrosis. Spearman's correlation was significant (r=0.5331, p<0.0001).

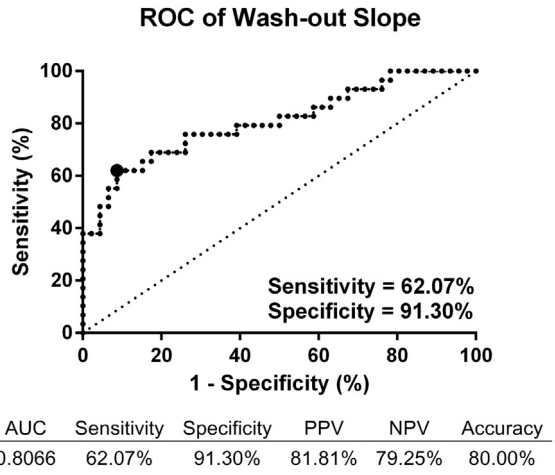

AUC	Sensitivity	Specificity	PPV	NPV	Accuracy
0.8066	62.07%	91.30%	81.81%	79.25%	80.00%

Figure 4 Receiver operating characteristic curve of the wash-out slope at the 180-second cut-off in distinguishing liver cirrhosis (Ishak stage F6) from non-cirrhosis (Ishak stages F0–F5). The AUC was 0.8066. The sensitivity was 62.07%, specificity was 91.3%, the positive predictive value (PPV) was 81.81%, negative predictive value (NPV) was 79.25%, and accuracy was 80%.

the hepatic sinusoids and the space of Disse when liver fibrosis develops. Therefore, the Marterne model may be accurate in the setting of normal liver parenchyma with free exchange between sinusoids and perisinusoidal space, but may not be accurate in fibrotic liver.[23] To solve this problem, Koh *et al.* introduced a dual-input, two-compartment model.[24] They assumed that the liver is composed of two compartments: one with well-perfused hepatic sinusoids and vascular space, and one with poorly perfused Disse and interstitial spaces. Both of the above models assume that the dual blood supplies to the liver can be approximated by extrahepatic segments of the hepatic arteries and portal veins; however, the extrahepatic segments of portal veins and hepatic arteries are not in the vicinity of the inlet of the hepatic sinusoids, and so it may not reflect the actual input

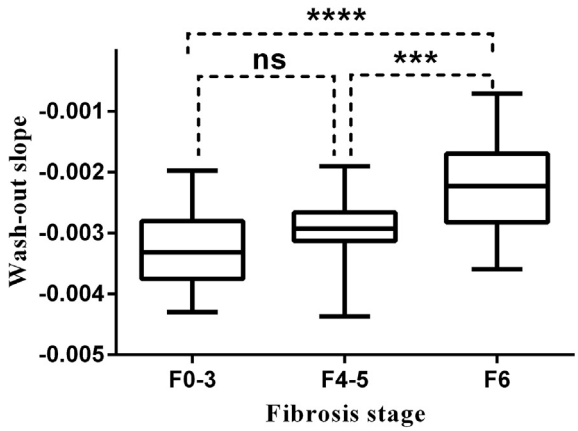

Figure 5 The mean, standard deviation, maximum and minimum plots of 180-second washout slopes at difference fibrosis stages. The difference between the F0–3 versus F6 and F4–5 versus F6 are significant (****p<0.0001 and ***p<0.001).

functions. Moreover, both models do not take into account the complex haemodynamic changes between the hepatic arteries and portal veins in liver cirrhosis,[25] such as hepatofugal portal blood flow, portal systemic shunting, and intrahepatic shunts.

To account for the limitations of fully quantitative methods, our semi-quantitative method has several advantages. First, it obviates the potential errors arising from measuring extrahepatic segments of hepatic arteries and portal veins as the input functions of hepatic inflow. Second, it directly measures the normalised characteristics of the time–intensity curve without invoking complicated tissue modelling. Thus, it is more easily implemented in clinical settings. Third, it requires very simple calculation to derive the wash-out slope, and so high interobserver and intra-observer reliabilities can be achieved.

In the present study, high temporally-resolved DCE-MRI was used to plot the time–intensity curve, from which the wash-in slope and wash-out slope were evaluated with high precision. Compared to the wash-out slope, the wash-in slope showed lower intra-observer and interobserver reliabilities. This may be due to the fact that the inflow ratios of the portal veins to the hepatic arteries vary across patients due to different levels of liver fibrosis,[14] and also they might vary spatially when liver fibrosis is inhomogeneous. In contrast, the wash-out of contrast medium (Gd-DTPA, used in this study) in the liver has only one system,[26] i.e., hepatic veins, and so the wash-out slope is relatively constant throughout the liver.

Early heterogeneous enhancement of the liver was commonly seen in MRI images from clinical practice.[27] The images indicated several types of chronic liver disease such as: hepatocyte necrosis, fibrosis, and inflammatory processes; however, liver enhancement was improved in later phase images. This may explain why wash-in curves had worse interobserver and intra-observer variability than wash-out curves. When ROIs were changed (different observers and different times), the wash-in curve also changed due to ROIs that cover the early heterogeneous enhancement zone. Furthermore, the wash-in curve is more easily changed not only due to liver fibrosis grade, but also liver inflammation processes (e.g., virus hepatitis and tumour inflammation) and minor focal necrosis of the hepatocytes.

Recently, transient elastography has been used to assess liver fibrosis by measuring liver stiffness. This ultrasound-based technique samples a cylindrical right lobe liver tissue of 4 cm long and 1 cm wide, approximately 2.5 cm below the skin.[28] Transient elastography is limited when liver fibrosis is inhomogeneous because it cannot assess the regions shadowed by the ribs. It is also limited in patients with thick subcutaneous fat, which attenuates the ultrasound beam before entering the liver. Similarly, MRI elastography only evaluates certain areas of liver that have adequate wave amplitude,[29] it must avoid areas vibrated by the beating heart, and is limited in the presence of ascites and high body mass index.[30] In contrast, DCE-MRI uses smaller ROIs than transient elastography, and is not hindered by the ribs and thick subcutaneous fat. Furthermore, DCE-MRI can exploit the whole liver by simply choosing different ROIs. Therefore, when the target area of non-tumour liver parenchyma is not suitable for MRI elastography or transient elastography, such as the left lobe liver,[31,32] DCE-MRI could serve as an alternative measurement.

There were seven patients excluded due to “enhancement failure” during the DCE-MRI scanning period. Four of the seven patients showed increased enhancement of liver parenchyma without any washout slope. Three of these seven patients showed a prolonged time-to-peak (>4.5 minutes) with a very short wash-out curve. In these patients, the bolus enhancement became a “dripping enhancement”. This may have been due to the small amount and slow flow of MRI contrast medium back to the heart; therefore, these patients as “enhancement failure”. Four additional patients were excluded due to “atypical enhancement” (outliers). Two were due to liver cirrhosis (F6) with sharp wash-in and wash-out slopes during repeated ROI evaluation, which may have been due to liver tumours or hepatitis increasing liver parenchyma enhancement. Two patients presented with liver fibrosis grade 3 and grade 5 with very slow wash-in and wash-out curves, which may have been due to delayed and prolonged contrast medium flow back to heart. The strengths of the present study include the use of surgical specimens instead of core biopsy samples for histological staging, and a simple analytical method that does not require input functions from the hepatic arteries and portal veins. The limitations of this study include small number of patients in each liver fibrosis stage, and potential errors of co-localisation between MRI measurement and pathological specimens, as the pathological specimens were not obtained under MRI guidance. To reduce the mismatch error between pathology and DCE-MRI study, the corresponding location in the liver could be marked using “blue dye” with a fine needle before liver resection. Then, pathologists could report the fibrosis grade at the marked location, and then imaging and pathology findings could be compared at the same location.

In conclusion, a practical method to evaluate liver fibrosis using DCE-MRI was proposed. The wash-out slope at the 180-second cut-off was found to be the most reliable, yielding a sensitivity of 62.07% and specificity of 91.3% in differentiating liver cirrhosis from non-cirrhosis. This parameter could potentially be useful in assessing liver cirrhosis for patients with Child’s A classification before hepatectomy, and warrants a longitudinal study for clinical validation.

Conflict of interest

The authors declare no conflict of interest.

Acknowledgements

This study was supported in part by Chang Gung Memorial Hospital (CMRPG6C0332). The authors thank colleagues in the Department of Clinical Research and Department of Pathology for providing helpful advice for this research.

References

1. Braet F, Wisse E. Structural and functional aspects of liver sinusoidal endothelial cell fenestrae: a review. *Comp Hepatol* 2002;**1**(1):1.
2. Schuppan D, Afdhal NH. Liver cirrhosis. *Lancet* 2008;**371**(9615):838–51.
3. Tsochatzis EA, Bosch J, Burroughs AK. Liver cirrhosis. *Lancet* 2014;**383**(9930):1749–61.
4. Zimmermann H, Reichen J. Hepatectomy: preoperative analysis of hepatic function and postoperative liver failure. *Dig Surg* 1998;**15**(1):1–11.
5. Pannu HK, Maley WR, Fishman EK. Liver transplantation: preoperative CT evaluation. *RadioGraphics* 2001;**21 Spec**:S133–46.
6. Seeff LB, Everson GT, Morgan TR, *et al*. Complication rate of percutaneous liver biopsies among persons with advanced chronic liver disease in the HALT-C trial. *Clin Gastroenterol Hepatol* 2010;**8**(10):877–83.
7. Scott DR, Levy MT. Liver transient elastography (Fibroscan): a place in the management algorithms of chronic viral hepatitis. *Antivir Ther* 2010;**15**(1):1–11.
8. Khalifa F, Soliman A, El-Baz A, *et al*. Models and methods for analyzing DCE-MRI: a review. *Med Phys* 2014;**41**(12):124301.
9. Tuncbilek N, Kaplan M, Altaner S, *et al*. Value of dynamic contrast-enhanced MRI and correlation with tumour angiogenesis in bladder cancer. *AJR Am J Roentgenol* 2009;**192**(4):949–55.
10. Essig M, Shiroishi MS, Nguyen TB, *et al*. Perfusion MRI: the five most frequently asked technical questions. *AJR Am J Roentgenol* 2013;**200**(1):24–34.
11. Drixler TA, Vogten MJ, Ritchie ED, *et al*. Liver regeneration is an angiogenesis- associated phenomenon. *Ann Surg* 2002;**236**(6):703–11. Discussion 711-702.
12. Thng CH, Koh TS, Collins DJ, *et al*. Perfusion magnetic resonance imaging of the liver. *World J Gastroenterol* 2010;**16**(13):1598–609.
13. Patel J, Sigmund EE, Rusinek H, *et al*. Diagnosis of cirrhosis with intravoxel incoherent motion diffusion MRI and dynamic contrast-enhanced MRI alone and in combination: preliminary experience. *J Magn Reson Imaging* 2010;**31**(3):589–600.
14. Hagiwara M, Rusinek H, Lee VS, *et al*. Advanced liver fibrosis: diagnosis with 3D whole-liver perfusion MR imaging—initial experience. *Radiology* 2008;**246**(3):926–34.
15. DCE MRI Technical Committee. *DCE MRI quantification profile QIBAVRDQ*. 30 July 2018. Available from: https://rsna.org/QIBA_.aspx.
16. Thevenaz P, Ruttimann UE, Unser M. A pyramid approach to subpixel registration based on intensity. *IEEE Trans Image Process* 1998;**7**(1):27–41.
17. Verma S, Turkbey B, Muradyan N, *et al*. Overview of dynamic contrast-enhanced MRI in prostate cancer diagnosis and management. *AJR Am J Roentgenol* 2012;**198**(6):1277–88.
18. Ishak K, Baptista A, Bianchi L, *et al*. Histological grading and staging of chronic hepatitis. *J Hepatol* 1995;**22**(6):696–9.
19. McGraw KO, Wong SP. Forming inferences about some intraclass correlation coefficients. *Psychol Meth* 1996;**1**:30–46.
20. Standish RA, Cholongitas E, Dhillon A, *et al*. An appraisal of the histopathological assessment of liver fibrosis. *Gut* 2006;**55**(4):569–78.
21. Calvaruso V, Burroughs AK, Standish R, *et al*. Computer-assisted image analysis of liver collagen: relationship to Ishak scoring and hepatic venous pressure gradient. *Hepatology* 2009;**49**(4):1236–44.
22. Materne R, Smith AM, Peeters F, *et al*. Assessment of hepatic perfusion parameters with dynamic MRI. *Magn Reson Med* 2002;**47**(1):135–42.
23. Banerji A, Naish JH, Watson Y, *et al*. DCE-MRI model selection for investigating disruption of microvascular function in livers with metastatic disease. *J Magn Reson Imaging* 2012;**35**(1):196–203.
24. Koh TS, Thng CH, Lee PS, *et al*. Hepatic metastases: *in vivo* assessment of perfusion parameters at dynamic contrast-enhanced MR imaging with dual-input two-compartment tracer kinetics model. *Radiology* 2008;**249**(1):307–20.
25. Kawasaki T, Moriyasu F, Kimura T, *et al*. Hepatic function and portal haemodynamics in patients with liver cirrhosis. *Am J Gastroenterol* 1990;**85**(9):1160–4.
26. Seale MK, Catalano OA, Saini S, *et al*. Hepatobiliary-specific MR contrast agents: role in imaging the liver and biliary tree. *RadioGraphics* 2009;**29**(6):1725–48.
27. Kanematsu M, Danet MI, Leonardou P, *et al*. Early heterogeneous enhancement of the liver: magnetic resonance imaging findings and clinical significance. *J Magn Reson Imaging* 2004;**20**(2):242–9.
28. Foucher J, Chanteloup E, Vergniol J, *et al*. Diagnosis of cirrhosis by transient elastography (FibroScan): a prospective study. *Gut* 2006;**55**(3):403–8.
29. Venkatesh SK, Yin M, Ehman RL. Magnetic resonance elastography of liver: technique, analysis, and clinical applications. *J Magn Reson Imaging* 2013;**37**(3):544–55.
30. Wagner M, Corcuera-Solano I, Lo G, *et al*. Technical failure of MR elastography examinations of the liver: experience from a large single-center study. *Radiology* 2017:160863.
31. Frulio N, Trillaud H. Ultrasound elastography in liver. *Diagn Interv Imaging* 2013;**94**(5):515–34.
32. Venkatesh SK, Yin M, Ehman RL. Magnetic resonance elastography of liver: clinical applications. *J Comput Assist Tomogr* 2013;**37**(6):887–96.